Fatigue notch sensitivity of steel blunt-notched specimens

M. D. CHAPETTI,[1] T. TAGAWA[2] and T. MIYATA[2]

[1]*INTEMA, University of Mar del Plata, J.B. Justo 4302 (B7608FDQ) Mar del Plata Argentina and* [2]*Material Science and Engineering, Nagoya University, Nagoya, 464-8603, Japan*

Received in final form 10 November 2001

ABSTRACT The notch sensitivity of three steels with similar plain fatigue limits was analysed and modelled. The analysis was made by using a model previously derived which estimated the fatigue limit of blunt notched components by means of the parameter k_{td} defined as the stress concentration introduced by the notch at a distance d from the notch root surface equal to the distance between microstructural barriers. The analyses show how the first two or three microstructural barriers define the fatigue limit and the fatigue notch sensitivity of blunt notched specimens.

Keywords blunt notches; fatigue limit; fatigue notch sensitivity; microstructural barriers.

INTRODUCTION

It is well known that two patterns of notch fatigue behaviour can occur in polycrystalline metals.[1–10] In 'sharp' notches (high stress concentration factor, k_t), mechanically short non-propagating cracks exist at the fatigue limit of the notched component, whereas 'blunt' notches (small k_t), exhibit microstructurally short non-propagating cracks. In the case of blunt notches the stress that is sufficient to initiate a crack at the notch root and overcome the strongest microstrucural barrier, is also sufficient to cause continuous propagation of the crack to failure and the fatigue strength is given by a microstructural threshold determined by a $\Delta\sigma$ criterion. On the other hand, in the case of sharp notches the fatigue strength is given by a mechanical threshold defined by a ΔK criterion, and the development of mechanical non-propagating cracks is allowed by the existence of a stress gradient high-enough and the development of the crack closure effect. In this case the fatigue strength becomes independent of the stress concentration factor k_t and is governed mainly by the notch depth D and the fatigue threshold $\Delta\sigma_{th}$ for physically small or long cracks.[4,7,8]

In a previous work,[11] a model for the notch size effect on the basis of the experimental evidence that both, the plain- and the blunt-notched fatigue limit represents the threshold stress for the propagation of the nucleated microstructurally short cracks, was derived. The derived relationship characterises the fatigue notch sensitivity by means of the parameter k_{td} defined as the stress concentration introduced by the notch at a distance d from the notch root surface equal to the distance between microstructural barriers, as follows:

$$k_{td} = \frac{k_t}{\sqrt{1 + \frac{4.5d}{\rho}}} \tag{1}$$

where ρ is the notch radius.

Defining d_i as the mean distance between microstructural barriers i, and $\Delta\sigma_{edi}$ as the fatigue limit associated to the same barrier i, the fatigue limit $\Delta\sigma_e$ of the notched component at a given k_t would be given by the greatest $\Delta\sigma_{edi}$ at that k_t, as follows:

$$\Delta\sigma_e|_{k_t} = \max\ \Delta\sigma_{edi}|_{k_t} = \max\left[\frac{\Delta\sigma_{e0di}\sqrt{1 + 4.5\frac{d_i}{\rho}}}{k_t}\right]_{k_t} \tag{2}$$

and

$$\Delta\sigma_{edi} = \frac{\Delta\sigma_{e0di}}{k_{tdi}} \tag{3}$$

where $\Delta\sigma_{e0di}$ is the effective resistance of the barrier i and k_{tdi} is the stress concentration introduced by the notch at a depth $x = d_i$. The concept is shown schematically in

Correspondence: M. D. Chapetti, INTEMA, University of Mar del Plata, J.B. Justo 4302 (B7608FDQ) Mar del Plata Argentina. E-mail: mchapetti@fi.mdp.edu.ar

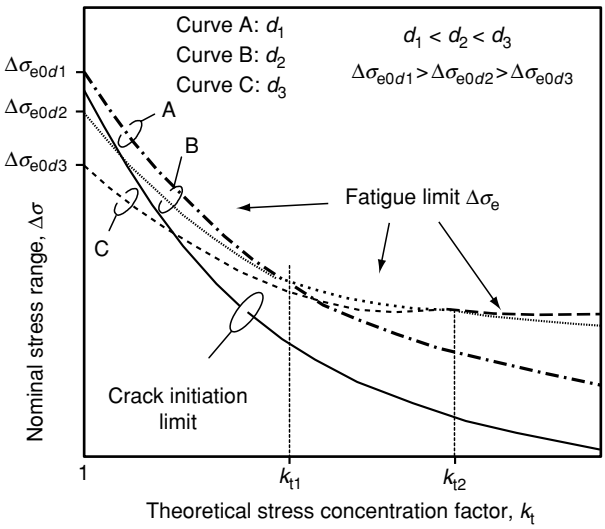

Fig. 1 The fatigue limit $\Delta\sigma_e$ of blunt notches defined as the greatest fatigue limit associated with the effective resistance $\Delta\sigma_{e0di}$ and the position from the notch-root surface d_i of the microstructural barriers i, see Eq. (3).

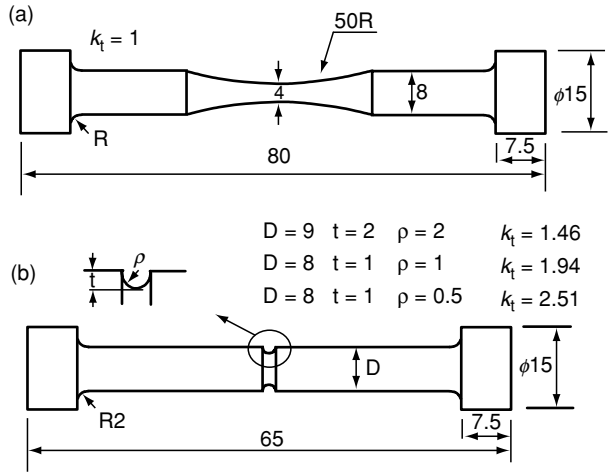

Fig. 2 Specimens, dimensions are in mm. (a) Smooth round bar specimen ($k_t = 1$); (b) Notched round bar specimen.

Fig. 1 by considering three consecutive microstructural barriers spaced at distances d_1, d_2 and d_3 from the surface ($d_1 < d_2 < d_3$), with their effective resistance $\Delta\sigma_{e0d1}$, $\Delta\sigma_{e0d2}$ and $\Delta\sigma_{e0d3}$, respectively. From $k_t = 1$ to k_{t1} the fatigue limit of the notch component is given by $\Delta\sigma_e = \Delta\sigma_{e0d1}/k_{td1}$, from k_{t1} to k_{t2} by $\Delta\sigma_e = \Delta\sigma_{e0d2}/k_{td2}$, and so on.

In this work this concept was used to analyse the influence of the position and the effective resistance of the microstructural barriers on the fatigue notch sensitivity of three steels with similar plain fatigue limits.

MATERIALS, SPECIMENS AND TESTING CONDITIONS

Three different steels were analysed. Their compositions and mechanical properties are shown in Tables 1 and 2, respectively. Steel A, JIS SW12-5, had a bainite-martensite microstructure. Steel B and C were Si and Cu solution hardened, respectively, and were obtained by laboratory remelting up to 1200 C and then hot rolled. They had a ferrite-pearlite microstructure. Steel C was then subjected to ageing treatment of 500 °C for 2 h. An increasing in 30% in tensile strength was observed by this treatment (Cu-precipitation hardening).

Four different bar tensile specimens were tested (see Fig. 2). One of them with plain surface while the other three with blunt notches. According to the results from finite element methods the values of the theoretical concentration factor k_t in notched specimens were 1.46, 1.94 and 2.51. After machining, the notches were mechanically polished with a series of grits down to 1 mm diamond paste. All fatigue test specimens were chemically etched in 3% Nital before being tested. The specimens were analysed after testing with a SEM.

Table 1 Chemical compositions of steels tested (wt%)

Steel	C	Si	Mn	P	S	Al	Cu
A	0.08	0.21	1.5	0.004	0.003	0.031	–
B	0.1	**1.96**	0.79	0.003	0.002	0.024	–
C	0.1	0.04	0.82	0.003	0.002	0.028	**1.56**

Table 2 Mechanical properties of steels tested

Steel	Microstructure	σ_{ys} (MPa)	σ_{uts} (MPa)	$\Delta\sigma_{e0}$ (MPa)	E.L. (%)	Hv
A	Bainite-Martensite	532	740	580	17.1	288
B	Ferrite-Pearlite Si-added	423	563	590	–	–
C	Ferrite-Pearlite Cu-added	512	646	600	25.6	214

Constant stress amplitude tests under axial loading with zero mean stress and 30 Hz frequency were carried out in an Instron fatigue test machine. All tests were performed at room temperature in laboratory air. The fatigue limit $\Delta\sigma_e$ was defined as the maximum nominal stress under which a specimen endured more than 10^7 cycles. The crack initiation limit $\Delta\sigma_i$ was defined as the limiting nominal stress required to obtain any microstructurally short crack at 10^7 cycles. Stress level was kept constant for each tested specimen. The fatigue limit $\Delta\sigma_e$ was then analysed by testing different specimens at different stress

levels. The stress increment between two consecutive stress levels was chosen equal to 10 MPa. Cracks observed at stress levels below the fatigue limit were considered as non-propagating cracks, and any possible further propagation was not analysed.

RESISTANCE AND POSITION OF THE MICROSTRUCTURAL BARRIERS

Figure 3(a–c) show the stress distributions ahead of the notch root corresponding to the notches analysed, according to Eq. (1) with the distance ahead of the notch root x instead of d, and for nominal stress ranges at and below the fatigue limit and above the initiation limit of the microstructures corresponding to the steel A, B and C, respectively. The effective resistance of the microstructural barriers was estimated by using these figures and the observations of non-propagating cracks obtained experimentally. The elastic stress distributions were drawn only to the depth given by the length of the longest arrested crack obtained at a given nominal stress level. In most of the cases (mainly for microstructurally short cracks) the depth a of the non-propagating cracks was defined by using the total surface length $2c$ and considering that the aspect ratio a/c was about 1 (semicircular cracks), which was observed experimentally by means of transverse cutting of some of the observed non-propagating cracks. When physically short non-propagating cracks were obtained, the specimens were fractured and the crack analysed and measured by using the SEM. Figure 4(a–c) show examples of the microstructurally short non-propagating cracks obtained for steels A, B and C, respectively.

Steel A (bainite-martensite microstructure – Fig. 3a)

In this microstructure the cracks initiate in the ferritic laths of the bundles, thus the size and the relative orientation of these bundles define the position and resistance of the first microstructural barrier ($d_1 = 50\,\mu$m and $\Delta\sigma_{e0d1} = 580$ MPa, approximately).[11] The position and resistance of the second and third barriers is given by the austenitic grain size: $d_2 = 120\,\mu$m with $\Delta\sigma_{e0d2} = 540$ MPa, and $d_3 = 240\,\mu$m with $\Delta\sigma_{e0d3} = 470$ MPa.

Steel B and C (ferrite-pearlite microstructures – Fig. 3b & c)

Stage I cracks usually initiate along the PSB proceeding in ferrite grains or along grain boundaries. In any case the grain boundaries are considered as microstructural

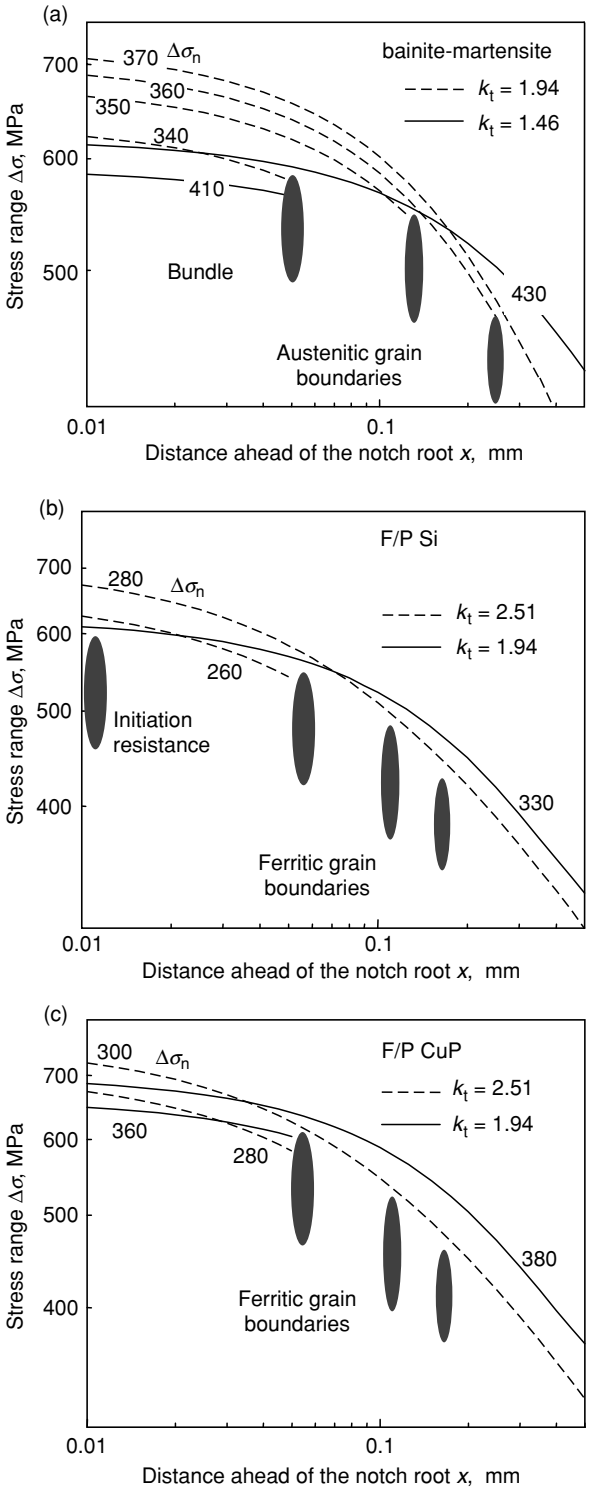

Fig. 3 Stress distributions ahead of the notch root for different nominal applied stress ranges and two stress concentration factors – from Eq. (1) with x instead of d. (a) bainite-martensite steel; (b) ferrite-pearlite Si-added steel; and (c) ferrite-pearlite Cu-added steel.

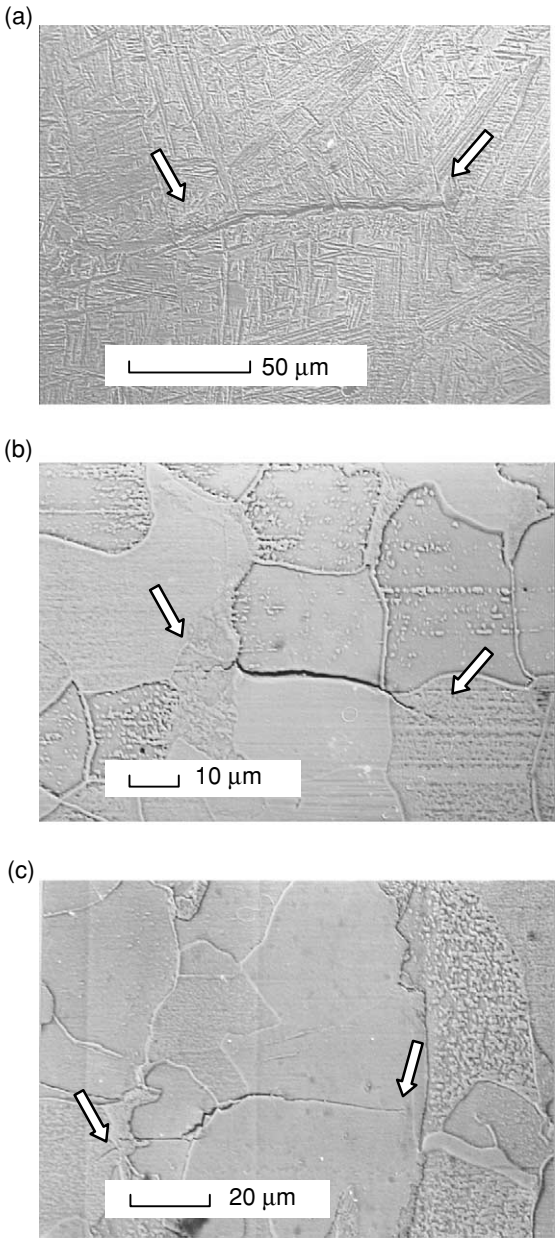

Fig. 4 Examples of the microstructurally short non-propagating cracks obtained in bainite-martensite steel (a); ferrite-pearlite Si-added steel (b); and ferrite-pearlite Cu-added steel (c).

barriers and the position given by the average size of the ferritic grains (about to 55 μm), is considered as the distance between two consecutive barriers. In this way we get $d_1 = 0.055\,\mu\text{m}$, $d_2 = 0.11\,\mu\text{m}$, $d_3 = 0.165\,\mu\text{m}$, and so on. The effective resistances of the barriers were estimated to be $\Delta\sigma_{e0d1} = 540\,\text{MPa}$, $\Delta\sigma_{e0d2} = 480\,\text{MPa}$, and $\Delta\sigma_{e0d3} = 425\,\text{MPa}$ in steel B, and $\Delta\sigma_{e0d1} = 600\,\text{MPa}$, $\Delta\sigma_{e0d2} = 515\,\text{MPa}$, and $\Delta\sigma_{e0d3} = 450\,\text{MPa}$ in steel C.

RESULTS AND DISCUSSION

Figure 5(a–c) show plots of the fatigue limit versus the stress concentration factor k_t, obtained experimentally for the steels A, B and C, respectively. The length of the non-propagating cracks obtained at several stress levels below the fatigue limit were specified. The bold lines correspond to crack initiation (Eq. (1) with $k_f = k_t$), and the dotted lines correspond to Eq. (3) for the first two important microstructural barriers. Experimental results are also shown. It can be seen that Eq. (3) fit reasonably well the experimental data.

Figure 6 shows the relationship between the stress concentration factor k_t and fatigue limit $\Delta\sigma_e$. All the fatigue limits were normalised by the ones for respective unnotched specimens, $\Delta\sigma_{e0}$. It can be seen that the notch sensitivity is clearly different for the three steels analysed. The highest notch sensitivity was found in steel B, where the fatigue limit is given by the initiation of a microcrack ($k_{td} = k_t$, $d = 0$). In this microstructure the solution hardening obtained with Si increases the crack initiation resistance beyond the effective resistance of the strongest microstructural barrier. The first microstructural barrier (defined as the ferritic grain boundary), starts to define the fatigue limit at a k_t equal to about 1.7. Its relatively low effective resistance does not decrease significantly the notch sensitivity for higher k_t. The resistance of the following microstructural barriers are also relatively low, and this can be related to the fact that the mechanical threshold in this steel is also relatively low, due mainly to a lower roughness induced closure.

In steel C the plain fatigue limit $\Delta\sigma_{e0}$ is given by the first microstructural barrier in almost the whole k_t range analysed, and the notch sensitivity is given by k_{td1} with $d_1 = 55\,\mu\text{m}$. As in steel B, the effective resistance of the second and third microstructural barriers are relatively low.

In steel B and C both, $\Delta\sigma_{e0}$ and $\Delta\sigma_i$ are increased by increasing the resistance of the ferritic crystal to the dislocation movement. The initiated microcracks follow grain boundaries or are able to grow through ferritic grains in directions that are perpendicular to the maximum tensile stresses. As a result of this behaviour a flatter fracture surface is obtained, giving rise to a lower roughness induced closure and so, a lower mechanical threshold.

In steel A, the notch sensitivity is the lowest one and the fatigue limit is given by the first, second or the third microstructural barrier, as k_t increases. In this microstructure ΔK_{th} is apparently greater than in the other two, so the effective resistance of the second and third microstructural barriers are higher. The laths are effective in guiding the cracks. The length of the laths or the

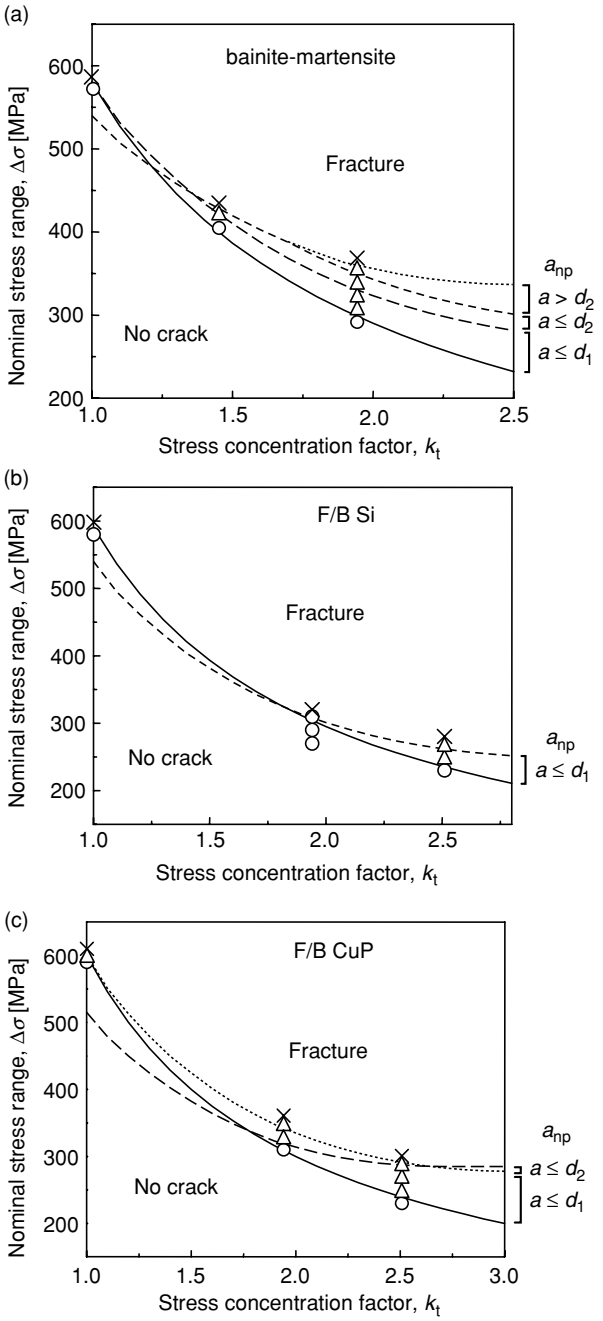

Fig. 5 Fatigue strength against theoretical stress concentration factor. ○ = No cracks, Δ = non-propagating cracks, × = fracture. (a) bainite-martensite steel; (b) ferrite-pearlite Si-added steel; and (c) ferrite-pearlite Cu-added steel.

size of the austenitic grain provide a relatively great d_1 and reduces the notch sensitivity. Besides, the orientation of the laths changes from one grain to another and, even though the effectiveness of these laths in guiding the cracks decreases as the crack length increases (as a result of an increasing in the driving force provided by ΔK), the cracks undergo important changes in directions and this generates relatively high roughness induced closure and

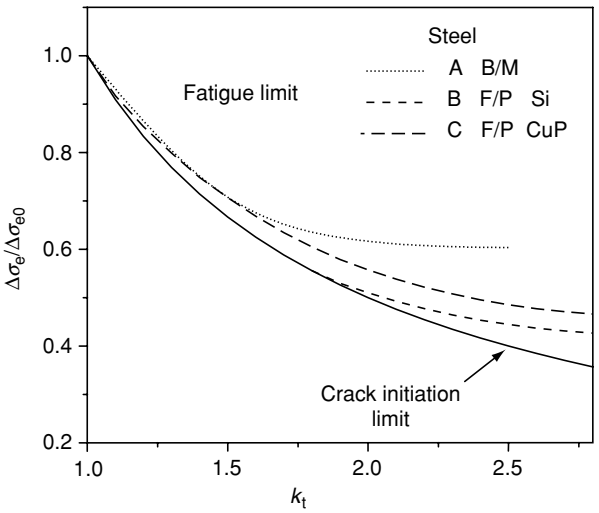

Fig. 6 Normalised fatigue limit against the theoretical stress concentration factor.

thus, a higher ΔK_{th}. As a result, a distribution of microstructural barriers with relatively high effective resistance is obtained, giving rise to an appreciable decreasing in the notch sensitivity as k_t increases.

In a previous paper,[12] the fatigue limit of blunt notched component was analysed from an energetic point of view. A total crack extension force was estimated by using both the local extension force, related with the surface strain concentration phenomena, and the external extension force given by the applied stress intensity factor. In the microstructurally small crack regime (i.e. for crack lengths in the same order of the critical microstructural dimension), the local crack extension force predominates, and thus the fatigue threshold is determined by the stress range $\Delta\sigma$ criterion and does not depend on ΔK. The critical or threshold stress, which represents the fatigue limit, is then given by the lowest stress range required to generate, by repeated cycling over a large number of cycles, the local strain fields which store enough energy to nucleate and drive the initiated small crack to fracture. If the extension force field is of the right magnitude but with insufficient range to overcome the microstructural barriers, a nucleated crack will eventually stop growing. However, continued cyclic deformation may generate the local field ahead of the crack (where the stress and the strains are larger) and then, if the external extension force is sufficient to aid its further growth, the crack could grow until it reaches the size for which the contribution of the external extension force predominates. It was shown that the effectiveness of the first microstructural barrier is mainly related to the local crack extension force. For the second barrier both, the local and the external extension forces have similar value, and for the third or deeper barriers (physically small cracks), the external crack extension force predominates.

In this case the non-propagating cracks are mainly given by a mechanical threshold defined by a ΔK criterion, and allowed by the existence of a stress gradient high-enough and the development of the crack closure effect.

According to the last concept, if the fatigue limit is associated with the third or fourth microstructural barriers, the amount of crack closure plays an important role and can explain the differences observed at relatively high k_t (2.51). Figure 7 shows the estimated distributions of the microstructural barriers for the three steels analysed. It can be seen that steels B and C have similar ΔK_{th}, and that for steel A it is relatively higher. The position of the microstructural barriers is given by the microstructural dimensions, and the distributions of their resistance are given by both, the intrinsic resistance to the local and the external extension force, and the development with crack depth of the extrinsic resistance (crack closure). Both, the microstructural dimensions (the position d of the barriers), and the material resistance (the resistance $\Delta\sigma_{e0d}$ of the barriers), are related and that is why it is usually a hard task to analyse one without changing the other. Probably the most simple assumption would be to consider d_1, $\Delta\sigma_{e0d1}$, ΔK_{th} and the development of the crack closure from $a = d_1$. Better estimations could be made considering the redistribution of stresses and the development of crack aspect ratio during crack growth. As we have mentioned in a previous work,[11] another important feature to take into account is the effect of mean stress, which depends on the mechanism responsible for crack propagation and the crack length. Further work will be conducted in this manner.

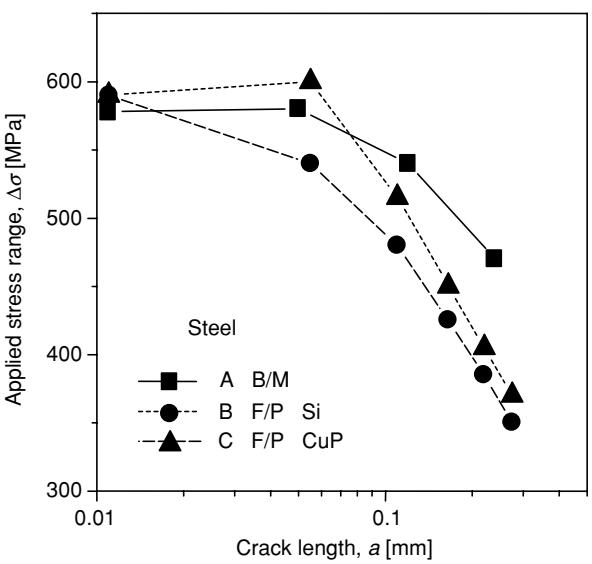

Fig. 7 Estimated distributions of the microstructural barriers for the three steels analysed. The position and the effective resistance of each barrier is characterised by a symbol.

CONCLUSIONS

The plain fatigue limit was given by the crack initiation resistance or by the first microstructural barrier. As the stress concentration effect increased, deeper barriers with lower effective resistance started to define the fatigue limit.

It was shown that not only the first and strongest barrier is important in defining the fatigue notch sensitivity, but also the distribution and the relative resistance of the second, third and so on, with respect to the first one.

Acknowledgements

One of the authors (M. D. Ch.) wishes to express his thanks for funding provided by the Consejo Nacional de Investigaciones Científicas y Técnicas (CONICET), and by Agencia Nacional de Promoción Científica de la Republica Argentina (PICTs 12-04585/6).

REFERENCES

1 Miller, K. J. (1993) The two thresholds of fatigue behaviour. *Fatigue Fract. Engng Mater. Struct.* **16**, 931–939.
2 Tanaka, K. and Nakai, Y. (1984) Prediction of fatigue threshold of notched components. *Transactions of the ASME* **106**, 192–199.
3 Smith, R. A. and Miller, K. J. (1978) Prediction of fatigue regimes in notched components. *Int. J. Mech. Sci.* **20**, 201–206.
4 El Haddad, M. H., Topper, T. H. and Smith, K. N. (1979) Prediction of non-propagating cracks. *Engng. Fract. Mech.* **11**, 573–584.
5 Lukás, P., Kunz, L., Weiss B. and Stickler, R. (1989) Notch size effect in fatigue. *Fatigue Fract. Engng Mater. Struct.* **12**, 175–186.
6 Tanaka, K., Nakai, Y. and Yamashita, M. (1981) Fatigue growth threshold of small cracks. *Int. J. Fract.* **17**, 519–532.
7 Dowling, N. E. (1979) Notched member fatigue life predictions combining crack initiation and propagation. *Fatigue Fract. Engng Mater. Struct.* **2**, 129–138.
8 McEvily A. J. and Minakawa, K. (1987) On crack closure and the notch size effect in fatigue. *Engng. Fract. Mech.* **28**, 519–527.
9 Tanaka, K. and Akiniwa, Y. (1988) Resistance-curve method for predicting propagation threshold of short fatigue cracks at notches. *Engng. Fract. Mech.* **30**, 863–876.
10 Ting, J. C. and Lawrence, F. V. (1993) A crack closure model for predicting the threshold stresses of notches. *Fatigue Fract. Engng Mater. Struct.* **16**, 93–114.
11 Chapetti, M. D., Kitano, T., Tagawa, T. and Miyata, T. (1998) Fatigue limit of blunt-notched components. *Fatigue Fract. Engng Mater. Struct.* **21**, 1525–1536.
12 Chapetti, M. D., Kitano, T., Tagawa T. and Miyata, T. (1999) Two small-crack extension force concept applied to fatigue limit of blunt notched components. *Int. J. Fatigue* **21**, 77–82.